Ethanolamine phosphate on the second mannose as bridge in GPI anchored proteins: Towards understanding inherited PIGG deficiency

Mizuki Ishida[1], Yuta Maki[2,3], Akinori Ninomiya[4], Yoko Takada[5], Philippe M Campeau[6], Taroh Kinoshita[1,5], Yoshiko Murakami[1,5*]

[1]Yabumoto Department of Intractable Disease Research, Research Institute for Microbial Diseases, Osaka University, Suita, Osaka, Japan 565-0871; [2]Department of Chemistry, Graduate School of Science, Osaka University, Toyonaka, Osaka, Japan 560-0043; [3]Project Research Center for Fundamental Sciences, Graduate School of Science, Osaka University, Toyonaka, Osaka, Japan 560-0043; [4]Central Instrumentation Laboratory, Research Institute for Microbial Diseases, Osaka University, Suita, Osaka, Japan 565-0871; [5]WPI Immunology Frontier Research Center, Osaka University, Suita, Osaka, Japan 565-0871; [6]Department of Pediatrics, CHU Sainte-Justine and University of Montreal, Montreal, QC, Canada, H3T 1C5

A corresponding author:
Yoshiko Murakami MD. PhD.
Yabumoto Department of Intractable Disease Research
Research Institute for Microbial Diseases, Osaka University
3-1 Yamada-oka, Suita, Osaka 565-0871, Japan
yoshiko@biken.osaka-u.ac.jp
tel +81-6-6879-8329
fax +81-6-6875-5233

Running title: Novel structure of GPI anchored proteins

Keywords
GPI transamidase, Mass spectrometry, PI-PLC

Abstract

Glycosylphosphatidylinositols (GPIs) are glycolipids that anchor many proteins (GPI-APs) on the cell surface. GPI precursor has three mannoses, which in mammalian cells, are all modified by the addition of ethanolamine-phosphate (EthN-P). It is postulated that EthN-P on the third mannose (EthN-P-Man3) is the bridge between GPI to the protein and the second (EthN-P-Man2) is removed after GPI-protein attachment. However, EthN-P-Man2 may not be always transient as postulated, as mutations of PIGG, the enzyme that transfers EthN-P to Man2, result in inherited GPI deficiencies (IGDs), characterized by neuronal dysfunctions. We hypothesized that EthN-P-Man2 plays a role beyond what is now postulated. Indeed, EthN-P on Man2 is not only the alternate bridge in some GPI-APs but the actual bridge in others, among them, the ect-5'-nucleotidase and netrin G2. We found that CD59, a GPI-AP, is attached via EthN-P-Man2 in both *PIGB*-knockout cells, in which GPI lacks Man3 and with a small fraction, in wild type cells. Our findings modify the current view of GPI anchoring and provide mechanistic bases of IGDs caused by *PIGG* mutations.

Introduction

Glycosylphosphatidylinositols (GPIs) are glycolipids found ubiquitously as membrane anchors of many proteins in eukaryotic organisms. The structures of GPI anchors were first determined in rat Thy-1 and trypanosome variant surface glycoprotein in the 1980s (1, 2), and shown that its backbone structure is highly conserved among all eukaryotes (3). Its basic structure is EthN-P-6-Man- α 1,2-Man- α 1,6-Man- α 1,4-GlcN- α 1,6-*myo*Inositol-phospholipid, where GlcN, Man, and EthN-P are glucosamine, mannose, and ethanolamine-phosphate respectively (1). This backbone is modified by various side chain groups in different organisms, or even in different proteins of the same organism. An example of the latter is mammalian GPI-APs, in which the first α 1,4-linked Man (Man1) is always modified by EthN-P side chain attached on the 2-position but a fourth Man may be attached to the third Man (Man3) via α 1,2-linkage.

GPI anchor precursors and precursor proteins are synthesized separately and assembly of GPI-anchored proteins (GPI-APs) occurs in the endoplasmic reticulum (ER). The GPI transamidase complex recognizes the C-terminal GPI attachment signal of precursor proteins (4), processes and attaches them to EthN-P on Man3 of GPI via an amide bond (5, 6). This EthN-P is thus called "bridging EthN-P". Both glycan and lipid moieties of GPI-APs are further modified in the ER and the Golgi before selectively trafficked to the cell surface. In mammalian cells, at least 27 genes, termed *PIG* (Phosphatidylinositolglycan) and *PGAP* (Post GPI attachment to proteins) genes, are

involved in the biosynthesis and maturation of GPI-APs (7).

In humans, more than 150 GPI-APs have been characterized, which functions include enzymes, receptors, adhesion molecules and complement regulatory proteins (8). Many of these GPI-APs and enzymes involved in their synthesis, play important roles in neuronal tissues. For instance, defects in *PIG* and *PGAP* genes cause inherited GPI deficiency (IGD), the main symptoms of which are intellectual disability, developmental delay, and seizures (9). At present, IGD caused by mutations in 22 genes involved in GPI biosynthesis (10-28) and the GPI-AP maturation pathway (29-31) have been reported. Defects in these genes lead mostly to embryonic death (32) but the vast majority of survivors, who show symptoms of IGD, have partial deficiencies in GPI biosynthesis. PIGO is an EthN-P transferase involved in attachment of the bridging EthN-P to Man3 (33), which is transferred by the mannosyltransferase PIGB to the GPI precursor (34). When analyzing HEK293 cells with the *PIGO* or *PIGB* gene knocked out (*PIGO*-KO or *PIGB*-KO), we unexpectedly found some GPI-APs, such as CD59 and DAF, which in turn were completely obliterated by further knockout of *PIGG.* PIGG is another EthN-P transferase involved in the attachment of the EthN-P to the second Man (Man2) in the precursor GPI (35), believed to be removed soon after GPI is attached to the precursor protein (36). The physiological significance of this transient modification has been unclear (35).

In *PIGG*-KO cells, GPI-APs such as CD59 and DAF, are normally transported and

expressed with the canonical structure. However, *PIGG* mutations in humans result in the mentioned IGD symptoms, suggesting an important role of PIGG in neuronal physiology (20, 37).

In this work, we analyzed by mass spectrometry, the GPI structure of CD59 expressed in *PIGB*-KO cells, and found that the EthN-P on Man2 is the bridging EthN-P. We also found CD59 with this same GPI structure in wild type HEK293 cells. It has long been postulated that in mammalian cells, the GPI-APs are always linked through the EthN-P on Man3. Our current data challenges this view.

Results

PIGG-dependent, low level expression of GPI-anchored CD59 and DAF in PIGO-KO and PIGB-KO cells.

It has been postulated that PIGG-dependent, Man2 linked EthN-P is a transient structure that is removed soon after attachment of protein to the Man3 linked EthN-P. In support of this notion is the similar expression levels of the GPI-APs, CD59 and DAF, observed in *PIGG*-KO HEK293 to those in non-mutated HEK293 (wild type) cells, as determined by fluorescence-activated cell sorting (FACS) analysis (Figure 1A). PIGO dependent Man3-linked EthN-P has been thought to act as the bridge in all GPI-APs (33). Unexpectedly, however, *PIGO*-KO HEK293 cells expressed, albeit low, clearly detectable levels of CD59 and DAF, being 6% and 19% of the levels observed in wild type

HEK293 cells, respectively (Figure 1B). Furthermore, the residual expression of CD59 as well as of DAF, completely disappears after further knockout of *PIGG* in *PIGO*-KO (*PIGO/PIGG*-DKO) cells, suggesting an important role of PIGG in the expression of these GPI-APs (Figure 1C). PIGO and PIGG are EthN-P transferases that add EthN-P to the 6-position of Man3 and Man2, respectively (33, 35). To test the possibility that PIGG compensated the PIGO loss and added the EthN-P to Man3 in *PIGO*-KO cells, PIGG was overexpressed in the *PIGO/PIGG*-DKO cells by transfection of *PIGG* cDNA (rescuer *PIGG*; Table S3). CD59 and DAF expression was restored up to, but not above, their levels in *PIGO*-KO cells (Figure 1C), suggesting a mechanism other than compensation by PIGG. Furthermore, in *PIGO*-KO cells, CD59 was slightly sensitive, and DAF completely resistant, to bacterial phosphatidylinositol-specific phospholipase C (PI-PLC) treatment, whereas in wild type cells both proteins were highly sensitive (Figure 1D), suggesting different structures in the GPI-anchors of these two GPI-APs in *PIGO*-KO vs wild type cells (see Discussion).

Furthermore, since Man3 is transferred by PIGB to Man2 in the α1,2 linkage way (34, 38), such transfer should not occur in *PIGB*-KO cells. Nevertheless, we observed low levels of CD59 and DAF in these cells, their levels being 3% and 7% to those in wild type cells, respectively (Figure 2A). In some cases, PIGZ transfers a fourth mannose (Man4) to Man3 in the same α1,2 linkage (39). Since *PIGB*-KO HEK293 cells express PIGZ, a possible explanation for the low expression of CD59 and DAF observed in these

cells is that PIGZ is compensating the missing PIGB function. However, further *PIGZ* knockout in *PIGB*-KO cells did not obliterate the low levels of CD59 and DAF (Figure 2B). And again, *PIGG* knockout in *PIGB*-KO cells resulted in the disappearance of the residual CD59 and DAF, further suggesting an important role of PIGG in the residual expression of these proteins (Figure 2C). In addition, differently to those in *PIGO*-KO cells, CD59 and DAF residually expressed in *PIGB*-KO cells were more sensitive to PI-PLC, especially CD59, of which about 90% became detached from *PIGB*-KO cells surface upon PI-PLC treatment (Figure 2D).

The results above strongly suggest that the EthN-P on Man2 is being used, albeit at a low efficiency, as bridge to CD59 and DAF.

Mass spectrometry (MS) reveals attachment of CD59 to Man2-linked EthN-P in PIGB-KO cells.

To determine the structural basis of PIGG-dependent CD59, we stably transfected HEK293 cells with the pME plasmid vector (40) expressing HFGF-CD59 (pME-puro-*HFGF-CD59*, the *CD59* cDNA fused to epitope tags and GST to aid in its purification, Table S3) and highly expressing cells were isolated by cell sorting. We then knocked out *PIGB* in these cells and isolated various cell clones. HFGF-CD59 proteins were solubilized by PI-PLC-treatment from both the original HEK293-*HFGF-CD59* cells and its *PIGB*-KO cell clones, followed by GST affinity purification, SDS-PAGE and in-gel

trypsin digestion (Figure S1). The C-terminal peptide of HEK293-HFGF-CD59 linked to GPI glycan from both HEK293-*HFGF-CD59* cells and their *PIGB*-KO cell clones, was then structurally analyzed by LC-ESI-MS.

In the HEK293-*HFGF-CD59* cells sampling, we found precursor ions corresponding to the C-terminal 11 amino acid peptide (DLCNFNEQLEN) linked to GPI with three Man and a HexNAc side chain (*m/z* 912.0^{3+} and 1367.5^{2+}, MW 2734.45) (Figures 3A and S2). Analyses by MS/MS showed a group of fragment ions diagnostic of GPI (Figures 3B; *m/z* 422^{+}, GlcN-Ino-P; 447^{+}, EthN-P-Man-GlcN; 707^{+} , EthN-P-Man-GlcN-Ino-P; 851^{+}, P-Man-Man-(EthN-P-)Man-GlcN; 869^{+}, Man-(EthN-P-)Man-GlcN-Ino-P; 1111^{+}, P-Man-Man-(EthN-P-)Man-GlcN-Ino-P; 1421^{+}, peptide-EthN; 1663^{+}, peptide-EthN-P-Man; 1825^{+}, peptide-EthN-P-Man-Man) clearly defining the structure, DLCNFNEQLEN-EthN-P-Man-Man-(EthN-P-)(HexNAc-)Man-GlcN-Ino-P- (Figure 3A). HexNAc corresponds to GalNAc in mammalian GPIs, as described (41). We also found precursor ions of *m/z* 966.0^{3+} and 1448.5^{2+} (MW 2895.0) corresponding to a GPI-peptide having one extra Hex. The Hex could correspond to either Man4 or Gal extension of the GalNAc side chain (Figure S2) (42). No other precursor ion corresponding to the C-terminal peptide, and having any other known GPI structure, such as one lacking the GalNAc side chain, was detected. Quantitative analysis of peak area of total ion chromatogram (TIC) of each fragment, showed that most, if not all, GPIs of HFGF-CD59 expressed in

wild type HEK293 cells have a GalNAc side chain and that nearly 40% of them had either Man4 or Gal extension (Figure S2).

In the *PIGB*-KO HEK293-*HFGF-CD59* cells sampling, we found precursor ions corresponding to the C-terminal 11 amino acid peptide linked to GPIs having two Man and a HexNAc side chain (*m/z* 858.0^{3+} and 1286.4^{2+}; MW 2572.31) as well as some bearing Hex extension (*m/z* 912.0^{3+}; MW 2734.45) (Figures 4A and S3). MS/MS analysis indicated not only the GPI diagnostic fragments (*m/z* 422^{+}, 447^{+}, 707^{+}, 1421^{+} and 1663^{+}) but also two fragments corresponding to P-Man-(EthN-P-)Man-GlcN (*m/z* 689^{+}) and peptide-EthN-P-Man-(EthN-P-)Man (*m/z* 1948^{+}) (Figure 4B). The P-Man-(EthN-P-)Man structure can only be derived from a GPI core with the protein attached to the EthN-P on Man2. Results of TIC analysis showed that most GPIs of HFGF-CD59 in *PIGB*-KO HEK293 cells have only two Man and the GalNAc side chain, with approximately 20% bearing the Gal extension (Figure S3).

A small fraction of HFGF-CD59 in HEK293-HFGF-CD59 *cells is attached to Man2-linked EthN-P in GPI.*

We next determined whether CD59 protein attachment to Man2-linked EthN-P occurs in wild type cells by reanalyzing the MS data of HFGF-CD59 expressed in the HEK293-*HFGF-CD59* cells. Specifically, we analyzed precursor ions of *m/z* 912.0^{3+} and 1367.5^{2+} (MW 2734.45, corresponding to HFGF-CD59 C-terminal peptide plus GPI containing

three Man, one EthN-P side chain and HexNAc). Indeed, fragment ions of *m/z* 689^{+} and 1948^{+} were found in precursor ions of *m/z* 1367.47^{2+} and 911.98^{3+}, respectively (Figure 5B and 5C), indicating that the C-terminal peptide of CD59 is attached to Man2-EthN-P, with the structure, peptide-EthN-P-(Man-)Man-(EthN-P-)(HexNAc-)Man-GlcN-PI (Figure 5A). These fragment ions were present in approximately 10% of precursor ions with MW 2734.45, which have three Man (data not shown). These results implicate that approximately 10% of CD59 with this newly discovered structural feature, were originally expressed in the HEK293-*HFGF-CD59* cells.

Expression of several GPI-APs are PIGG dependent and preferentially bridged through Man2-linked EthN-P.

The previous results showing that approximately 10% of HFGF-CD59 are bridged through Man2-linked EthN-P in HEK293 cells transfected with the tagged *HFGF-CD59* gene, suggest the possibility that some GPI-APs are preferentially linked in this way (Figure S4). If this is true, the expression of these proteins might be lower in *PIGG*-KO cells than in wild type cells. To test this hypothesis, GPI-APs were isolated from wild type and two clones of *PIGG*-KO HEK293 cells, by a combination of repeated Triton X114 phase separation and a PI-PLC treatment (Figure 6). The isolated proteins were then analyzed by LC-ESI-MS/MS and a total of 36 GPI-APs identified (Table S1). Of these, seven GPI-APs (tissue-nonspecific alkaline phosphatase (ALPL), ciliary

neurotrophic factor receptor (CNTFR), contactin1 (CNTN1), melanotransferrin (MELTF), ecto 5'-nucleotidase (NT5E or CD73), reversion-inducing-cysteine-rich protein with kazal motifs (RECK), and reticulon 4 receptor like 2 (RTN4RL2)), were lower in the two *PIGG*-KO cloned cells than in wild type HEK293 cells (Table S1), as determined by comparative measurements using the Scaffold4 software (43).

To confirm these results, cell surface levels of the GPI-APs were also analyzed by FACS. Observed levels of NT5E (43.8±11.0% of wild type level, n=4) and EphrinA5 (53.7±10.0%, n=3) were lower in the *PIGG*-KO (Figure 7A). No changes in the levels of CD109, DAF or CD59 were observed (Figure 7A). The reduced level of NT5E, but not that of EphrinA5, on *PIGG*-KO cells was rescued by transfection of *PIGG* cDNA (Figure 7B). Furthermore, the cell surface levels of CD109, DAF, CD59, MELTF and prion protein (PRNP) on *PIGG*-KO cells did not increase upon transfection of *PIGG* cDNA (Figure 7B). These results show that the GPI-APs, which were rescued by transfection of *PIGG* cDNA, are PIGG dependent and preferentially bridged through the Man2-linked EthN-P.

To further test if expression of other GPI-APs are similarly PIGG-dependent, various GPI-APs genes were HA-tagged and cloned using the *pME* expression vector. Genes of fifty GPI-APs, known to be expressed in the brain, were selected and cloned for this work, and each recombinant plasmid co-transfected with *PIGG* cDNA, or an empty vector as control, into *PIGG*-KO HEK293 cells, followed by FACS analysis of the proteins expressed on the cell surface (Figure S5A and B). Expression levels of 18 of the

GPI-APs including ALP, CNTFR, CNTN1, RECK, NT5E, and glypican 3 (GPC3), were clearly lower in the *PIGG*-KO transfectants as compared to the *PIGG* cDNA rescued transfectants (Figure S5A) whereas those of 32 other GPI-APs were similar, or only slightly lower (Figure S5B). Repeated measurements on 14 out of the former group of 18 GPI-APs resulted in levels between 28.3±7.6 % and 62.5±13.8 % in *PIGG-KO* cells compared to *PIGG* cDNA rescued cells, while levels of 4 GPI-APs in the latter group of 32 were between 68.0±6.0 % and 88.1±3.9 % (mean±SD) (Figure 8A). These results indicate that the expression of the 18 GPI-APs tested is partially PIGG dependent and the extent of PIGG dependency varies among the proteins. Of those, Netrin G2 (NTNG2) was the most PIGG-dependent, showing approximately 70% reduction in *PIGG*-KO cells (Figure 8B). In other words, this *PIGG* dependency indicates that many GPI-APs, to varying degrees, are preferentially linked to Man2-linked EthN-P.

Establishment of a more sensitive and simpler functional assay for PIGG mutants found in individuals with IGD.

The results shown above of PIGG dependent residual expression of some GPI-APs (Figure 1C), lead us to propose a simpler method for assaying *PIGG* mutations, without using any radioactive material, based on the following: Using *PIGO/PIGG* DKO cells, PIGG activity was measured by transfecting *PIGG* cDNA followed by FACS analysis. *PIGG* cDNA transfection rescues the expression of GPI-APs to the levels of *PIGO*-KO

cells whereas a *PIGG* cDNA with R669C mutation (20) only partially rescues the expression of CD59 (Figure 9), probably due to decreased activity of the PIGG-R669C. The activity of R669C-PIGG was assessed by labelling with [^{14}C]-mannose PIGG-dependent GPI precursor and the radioactive product analyzed by thin layer chromatography (20). The procedures we have developed here for measuring PIGG activity, without using any radioactive material, which requires complex facilities and highly trained personnel, suggested us to establish a simpler method for measuring this protein activity and may be further developed for the prognosis of individuals with *PIGG* mutations.

Discussion

The core structure of GPI-APs is conserved among eukaryotes and it has been postulated that these proteins are always attached via EthN-P on Man3. In this study, we demonstrate the presence of a structural feature in GPI-APs not described before, in which EthN-P on Man2 bridges GPI anchor to proteins. We initially found that the residual expression of GPI-APs in *PIGB*-KO cells and *PIGO*-KO HEK293 cells are PIGG dependent (Figures 1 and 2). GPIs in *PIGB*-KO cells, which have only two mannoses, are attached to proteins via EthN-P linked to Man2 (Figure 4). Furthermore, we found that GPI with three mannoses and attached to a protein via EthN-P on Man2, is normally present in wild type HEK293 cells (Figure 5).

It is not yet known whether this alternative mode of protein attachment to GPI occurs in non-mammalian organisms. In organisms such as *Trypanosoma brucei*, in which only the Man3 is modified by EthN-P (44), this alternative mode of attachment may not occur. It has been reported that GPI core of *Entamoeba histolytica* proteophosphoglycan contains two mannoses and one galactose (45). The authors suggest that the galactose might act in place of the Man3 and the bridging EthN-P might be linked to the galactose. In view of our findings, an alternative interpretation is that the galactose is only a side chain and the bridging is through EthN-P linked to Man2. Similarly, various GPIs purified from *Babesia divergens*, a protozoan parasite, contain a maximum of two mannoses (44). Further analyses of the GPI structure of GPI-APs on these protozoan parasites are warranted.

We used HFGF tagged CD59 to demonstrate protein attachment to EthN-P on Man2. Approximately 10% of the tagged CD59 overexpressed in wild type HEK293 cells had the alternative mode of attachment to GPI, as estimated by MS data analysis. Using a newly developed method of GPI-AP isolation combined with a proteomic analysis (Figure 6), we detected 36 GPI-APs in HEK293 cells (Table 1). Seven of them, ALPL, CNTFR, RECK, CNTN1, MELTF, NT5E/CD73, and RTN4RL2, were clearly decreased in two independent clones of *PIGG*-KO cells (Table1). Decreased expression of NT5E in the *PIGG*-KO cells was rescued with *PIGG* cDNA (Figure 7). Among 50 GPI-APs known to be expressed in brain cells, many were highly, albeit not completely, PIGG-dependent

(Figure 8), indicating that the alternative mode of GPI-anchor bridged by Man2-linked EthN-P is not a rare exception but occurs widely in many GPI-APs to various extent.

The present results suggest causal relationship of GPI alternative bridging to *PIGG* mutations in IGD. Bi-allelic loss of function in *PIGG* mutations, found in individuals with IGD, may cause null or greatly decreased function of PIGG (20). It is likely therefore, that levels of a number of GPI-APs on the affected individuals' cells are decreased. Consistent with this, lower levels of several GPI-APs in fibroblasts from two siblings with a homozygous nonsense *PIGG* variant, have been reported (37). Reduced levels of specific GPI-APs may result in the clinical symptoms associated with *PIGG*-IGD, such as developmental delay, intellectual disability, seizures and hypotonia. Among GPI-APs potentially decreased in PIGG-defective neuronal cells, is NTNG2, which is deeply dependent upon *PIGG* (Figure 8). Recently, loss-of-function mutations in NTNG2, which is selectively expressed in presynaptic region, were found in several families, whose homozygous members showed global developmental delay, severe intellectual disability, muscle weakness, and behavioral abnormalities like Rett syndrome (46, 47). All these symptoms overlap with those of *PIGG*-IGD (20, 37). Likewise, NT5E/CD73, which is widely expressed in brain tissue cells, might account for some of brain related abnormalities. This enzyme is known to convert AMP to adenosine. Functions of NT5E/CD73 in the central nervous system include roles in locomotion and behavior, memory and plasticity, sleep regulation, and

thermoregulation (48).

GPI transamidase complex, consisting of PIGK, GPAA1, PIGT, PIGU, and PIGS (49-52), catalyzes the cleavage of the C-terminal signal peptide of GPI precursor proteins between the ω and ω+1 amino acids, and the formation of an amide bond between the ω amino acid carboxyl group and EthN of GPI. The catalytic subunit, PIGK is a cysteine protease that cleaves the C-terminal peptides and forms a carbonyl intermediate (49). GPAA1 has sequence homology to an M28 family peptide-forming enzyme, which catalyzes the formation of an amide bond between the carboxyl group of ω amino acid and amino group of EthN (50). Other crucial questions on how this complex function still remain, for instance, in wild type cells, how it selects the target EthN-P on Man2 or Man3? It seems that some precursor proteins set the preference to the Man2-linked EthN-P. It is possible that conformation of the enzyme complex changes depending upon the precursor protein, setting the target preference. Because PIGG deficiency mainly causes neurological defects, it is possible that GPI-APs in brain have the alternative mode of GPI attachment happening more frequently than those in other tissues/organs.

The question, what could be the functional difference between the two structures of GPI-APs, remains, which leads to other questions as to why and how PIGG deficiency causes the various neurological symptoms (20, 37). We found decreased levels of many GPI-APs in *PIGG*-KO cells. The decreased levels of these proteins in brain of PIGG deficient individuals, may be the cause of their various symptoms. On the other hand,

there must be a reason why some proteins are expressed with this alternative structure. Each GPI-AP works as a receptor, a ligand, an adhesion molecule, or as an enzyme. It is very possible that binding partners end up with different binding affinities to the GPI-APs with the alternate structure, resulting in altered biological processes, and hence neurological abnormalities.

In support of alterations in biological processes by PIGG deficiency, in yeast, *PIGG*-KO cells show growth defect and it is reported that the rate of ceramide replacement in the lipid moiety of GPI anchors is reduced, the transport of GPI-APs to the Golgi is delayed, and cell separation is disturbed (53).

Soon after the attachment of GPI to a precursor protein, the acyl chain linked to the inositol ring is usually removed by the GPI-deacylase PGAP1 (54). If removal of the acyl chain is prevented, the GPI-AP becomes PI-PLC resistant. CD59 in *PIGO*-KO cells is completely resistant to PI-PLC, even with overexpression of *PGAP1* (results not shown), whereas in *PIGB*-KO cells it is partially sensitive, albeit less sensitive as compared to that in wild type cells. PI-PLC does not act on CD59 expressed in *PIGO*-KO cells most likely because PGAP1 does not remove acyl chain from inositol in GPI, due to Man2-linked EthN-P as protein attachment and Man3 lacking EthN-P. In contrast, CD59 on *PIGB*-KO cells is partially sensitive to PI-PLC. This suggests that even when GPI has Man2-linked EthN-P being used in protein attachment, if Man3 is absent, PGAP1 acts on inositol-linked acyl chain. It is possible that PGAP1 recognizes these parts of GPI

around Man2 and Man3 during its deacylating action. From the proteomic analysis, it seems that PI-PLC sensitivity has no direct relation to the alternate structure of GPI-APs but rather to the inherent differences of PI-PLC sensitivity of different GPI-APs. It is also known that PI-PLC sensitivities of these proteins are different depending on their cell type origin. For instance, GPI-APs in red blood cells are completely resistant to PI-PLC as they are not deacylated from inositol by PGAP1 (55). PGAP1 activity is reported to have close association with ER stress (56). Under ER stress conditions, misfolded GPI-APs accumulate in the ER and deplete the available PGAP1, resulting in the exit of normal GPI-APs from the ER without being processed by PGAP1 (56). What structure is recognized by PGAP1 and how PGAP1 activity is regulated under non-stressed conditions, as well as the resulting GPI-APs sensitivities to PI-PLC under these conditions, are worth being clarified in the future.

Lastly, with the techniques we used for obtaining data on PIGG related effects, we propose a method to assess PIGG activity that is simpler and more sensitive. Previously, the activity of PIGG could only be determined by metabolic labelling of *PIGG* cDNA-transfected cells with radioactive mannose (^{14}C-mannose) and measuring the GPI intermediate bearing EthN-P on Man2 by thin layer chromatography and phosphorimaging (20). This method is time consuming and requires special facilities and training in radioisotope use. An example of the techniques we used are the ones for detecting residual expression of GPI-APs in *PIGO*-KO cells. PIGG activity on GPI-APs

can be measured by transfecting wild type or mutant *PIGG* cDNA into *PIGO/PIGG*-DKO cells, followed by FACS analysis. These are standard cellular and biochemical techniques, being relatively simple and sensitive (Figure 9). This new method can be further developed for more easily and accurately determine pathogenic effects of *PIGG* gene variants found in individuals with IGD.

In conclusion, we demonstrated that some GPI-APs are connected to the EthN-P on Man2 of GPI, instead of the postulated Man3, and suggest that this newly discovered alternative mode of GPI attachment is relevant in neurological development and functions.

Methods

Knockout (KO) cells

PIGO-, PIGB-, and *PIGG*-KO cells were generated from HEK293 cells using the CRISPR/Cas9 system (57). *PIGO/PIGG* and *PIGB/PIGG* double knockout (DKO) cell clones were generated by knocking out *PIGG* in cloned *PIGO-* and *PIGB*-KO cells, respectively. *PIGB/PIGZ* -DKO cells were generated by knockout of *PIGZ* in the cloned *PIGB*-KO cells. A pX330 plasmid for expression of the human codon-optimized *Streptococcus pyogenes* (Sp) Cas9 and chimeric guide RNA was obtained from Addgene (Cambridge, MA). The seed sequences for the SpCas9 target site in target genes are shown in Table S2. A pair of annealed oligos designed according to these sequences are

inserted into the BbsI site of pX330. HEK293 cells were transfected with pX330 containing the target site using Lipofectamine 2000 (Invitrogen, Carlsbad, CA). Knockout clones were obtained by limiting dilution and KO confirmed by sequencing the target sites in the genome DNA and by flow cytometric analysis of GPI-APs. For the rescue experiments, N or C-terminal tagged human *PIGO, PIGB, PIGG*, and *PIGZ* cDNAs were cloned into the mammalian expression vector, pMEpuro18sf+ (40), generating pME-puro-3HA-hPIGO, pME-puro-3HA-hPIGB, pME-puro-hPIGG, pME-puro-hPIGZ-3HA, respectively (Table S3).

Flow cytometry

Surface expression levels of GPI-APs were determined by staining cells with mouse anti-decay accelerating factor (DAF; clone IA10), -CD59 (clone 5H8) or -HA (clone HA-7, Sigma-Aldrich) followed by a PE-conjugated anti-mouse IgG antibody (BD Biosciences, Franklin Lakes, NJ). Cells were examined in the flow cytometer MACSQuantVYB (Miltenybiotec, Germany) and data analyzed with the Flowjo software (v9.5.3, Tommy Digital, Tokyo, Japan).

Generation of PIGB-KO cells expressing His-FLAG-GST-FLAG tagged CD59 (HFGF-CD59)

Wild type HEK293 cells were stably transfected with pME-puro-HFGF-CD59 and

highly expressor cells were sorted after labeling with anti-CD59. *PIGB-KO* cell clones were generated from these cells using CRISPR/Cas9 system, as described above. From the HFGF-CD59-expressing *PIGB*-KO cells, *PIGB/PIGZ*-DKO cells were further generated.

Purification of HFGF-CD59

Cells ($1x10^8$) stably expressing HFGF-CD59 were treated with 0.05 units/ml of phosphatidylinositol-specific phospholipase C (PI-PLC) (ThermoFisher, P6466) in 10 ml of PI-PLC buffer (Opti-MEM containing 10mM HEPES-NaOH, pH 7.4, 1 mM EDTA and 0.1% BSA) at 37 °C for 1 h. After centrifugation at 400 g for 5 minutes, the supernatant was loaded to a column of 500 μl of Glutathione Sepharose 4B at 4 °C. After washing repeatedly with a total of 10 ml PBS, protein was eluted with 5 ml of elution-buffer A (PBS containing 30 mM HEPES-NaOH, pH7.4, and 20 mM reduced glutathione). Protein in the eluted solution was precipitated with four volumes of acetone at -80 °C for 1h. After centrifugation at 13,400 x g for 30 min at 4 °C, the pellet was air dried dissolved in NuPAGE LDS Sample Buffer with reducing agent (Invitrogen). The protein pellet was further purified by electrophoresis in the Bolt 4-12% Bis-Tris Plus gel (Invitrogen), the gel stained with Imperial Protein Stain (Thermo Fisher Scientific) and a gel slice with the corresponding HFGF-CD59 protein excised.

Mass spectrometric (MS) analysis

The gel slice with the HFGF-CD59 protein was reduced with 10mM dithiothreitol (DTT), followed by alkylation with 55mM iodoacetamide, and in-gel digestion with trypsin. The resultant peptides were subjected to MS analysis by LC-ESI system. Data were obtained by nanocapillary reversed-phase LC-MS/MS using a C18 column (0.1 x 150 mm) on a nanoLC system (Advance, Michrom BioResources) coupled to an LTQ Orbitrap Velos mass spectrometer (Thermo Fisher Scientific). The mobile phase consisted of water containing 0.1% formic acid (solvent A) and acetonitrile (solvent B). Peptides were eluted with a gradient of 5–35% solvent B for 45 min at a flow rate of 500 nl/min. The mass scanning range of the instrument was set at *m/z* 350–1500. The ion spray voltage was set at 1.8 kV in the positive ion mode. The MS/MS spectra were acquired by automatic switching between MS and MS/MS modes (with collisional energy set to 35%). Helium gas was used as collision gas. In-house MASCOT Server (Matrix Science) and Xcalibur Software (Thermo Fisher) were used for analysis of mass data. In the MS/MS profiles, those that contained characteristic fragments derived from GPI anchors, such as fragment ions of *m/z* 422^+ and 447^+, were selected, and fragments in the selected profiles were assigned to determine the GPI structures. Based on the profiles of the MS/MS fragments, the peak areas of the parental MS fragments corresponding to predicted GPI-peptides were measured in total ion chromatogram and the ratio in the total GPI peptide fragments calculated.

Proteomics analysis of wild or *PIGG*-KO HEK293 cells

As shown in Figure 6, wild type and two *PIGG*-KO clones (#10, #4) of HEK293 cells ($5x10^6$ cells each) were lysed in 500 μl of lysis buffer (10 mM Tris-HCl, pH 7.4, 150 mM NaCl, 5 mM EDTA, protease inhibitor cocktail) containing 2% Triton X-114 (Nakalai Tesque, Kyoto, Japan) for 30 min on ice. After centrifugation at 15,000 rpm at 4°C for 15 min, the supernatant was incubated for 10 min at 37°C and aqueous and detergent phase separation was performed by centrifugation at 5,600g at 37°C for 7 min. After recovering the aqueous phase, 350 μl of lysis buffer added to the detergent phase and further incubated with PI-PLC (1 unit/ml) at 16 °C for 2h. Phase separation was performed and the aqueous phase combined with the previously recovered aqueous phase. Four volumes of acetone were added to the combined aqueous phase as well as to the detergent phase, and protein precipitation performed at -80 °C for 1h (Figure 6). Protein precipitate were pelleted by centrifugation at 13,400 x g for 30 min at 4 °C and the air dried. The air dried pellet was dissolved in 20 μl of 0.1% RapiGest (Waters) and reduced with 10 mM DTT, followed by alkylation with 55 mM iodoacetamide, digestion with trypsin and purification with a C18 tip (AMR, Tokyo, Japan). The purified peptides were subjected to nanocapillary reversed-phase LC-MS/MS analysis using a C18 column (10 cm x 75 um, 1.9 μm, Bruker Daltonics, Bremen, Germany) in a nanoLC system (Bruker Daltonics) connected to a timsTOF Pro mass spectrometer (Bruker Daltonics)

and a modified nano-ESI source (CaptiveSpray; Bruker Daltonics). The mobile phase consisted of water containing 0.1% formic acid (solvent A) and acetonitrile containing 0.1% formic acid (solvent B). Linear gradient elution was carried out from 5% to 30% solvent B for 18 min at a flow rate of 500 nL/min. The ion spray voltage was set at 1.6 kV in the positive ion mode. Ions were collected in the trapped ion mobility spectrometry (TIMS) device over 100 ms and MS and MS/MS data collected over an *m/z* range of 100–1,700. During the collection of MS/MS data, the TIMS cycle was adjusted to 0.53 s and included 1 MS plus 4 parallel accumulation serial fragmentation (PASEF)-MS/MS scans, each containing on average 12 MS/MS spectra (>100 Hz) (58, 59). Nitrogen gas was used as collision gas.

The resulting data was processed using DataAnalysis version 5.2 (Bruker Daltonics), and proteins identified using MASCOT version 2.6.2 (Matrix Science, London, UK) against the SwissProt database. Quantitative values were calculated with Scaffold4 (Proteome Software, Portland, OR, USA) for MS/MS-based proteomic studies (43).

Determination of expression levels of GPI-APs in PIGG-KO cells

GPI-APs were HA-tagged by cloning their coding cDNA amplified from the human cDNA library or from Invitrogen plasmids, as described (60), into the mammalian expression vector (pME-puro) and co-transfected into the *PIGG*-KO cells with *PIGG* cDNA or the empty vector as control. The expression levels of the GPI-APs were

determined by flow cytometric analysis

Acknowledgments

We thank Junji Takeda (Osaka University) and Mike Ferguson (University of Dundee) for discussion, Luiz Shozo Ozaki (Virginia Commonwealth University) for discussion and manuscript editing, Shota Nakamura and Daisuke Motooka (Osaka University) for running the next generation sequencer, Hideki Nakanishi (Jiangnan University) for offering us the plasmids, Keiko Kinoshita, Saori Umeshita, and Kae Imanishi (Osaka University) for technical help. This work was supported by JSPS and MEXT KAKENHI grants (JP16H04753 and JP17H06422 for T. Kinoshita), a grant from Ministry of Health, Labor and Welfare and a grant from Practical Research Project for Rare/Intractable Diseases from the Japan Agency for Medical Research and Development (AMED) (JP19ek0109418 for Y. Murakami).

Author contributions

MI, PC, TK and YoM designed the study, MI, YuM, AN, YT and YoM acquired the data and conducted experiments. MI, PC, TK and YoM wrote the paper.

Competing Interest Statement

The authors declare no conflicts of interest.

The paper Explained

PROBLEM

Glycosylphosphatidylinositols (GPI) serves as membrane anchor for about 150 proteins on the cell surface and play a variety of roles in the cell as hydrolytic enzymes, adhesion molecules, receptors, protease inhibitors, and complement regulatory proteins. GPI precursor has three mannoses, which in human cells are all modified by ethanolamine-phosphate (EthN-P). It is postulated that the EthN-P on the third mannose always bridges GPI to the protein, while that on the second is removed after GPI attachment. The role of this transient modification has not been elucidated. Consistently, several GPI-anchored proteins are not appreciably reduced in cells depleted of PIGG, the enzyme that transfers EthN-P to the second mannose. Nevertheless, Inherited PIGG deficiency, caused by the mutations in *PIGG* gene shows various neuronal abnormalities such as intellectual disability, interactable seizures and sometimes shows mitochondrial dysfunction.

RESULTS

We analyzed the GPI anchor structure of CD59, a GPI anchored protein, by mass spectrometry and found the novel GPI structure in which EthN-P on the second mannose bridges the protein. In addition, we showed that EthN-P on the second mannose is the preferential bridge for many other GPI-anchored proteins. Various

abnormalities in inherited PIGG deficiency would be caused by the defect in this structure.

IMPACT

Our findings modify current view of GPI anchors and provide mechanistic bases for understanding the effects of *PIGG* mutations.

For More Information

Disease HP of inherited GPI deficiency

http://igd.biken.osaka-u.ac.jp/en/

Data availability

The mass spectrometry proteomics data have been deposited to the ProteomeXchange Consortium via the PRIDE (61) partner repository with the dataset identifier PXD021996 and PXD022032 (project name, "A novel structure of GPI anchored proteins")

References

1. S. W. Homans *et al.*, Complete structure of the glycosyl phosphatidylinositol membrane anchor of rat brain Thy-1 glycoprotein. *Nature* **333**, 269-272 (1988).
2. W. J. Masterson, T. L. Doering, G. W. Hart, P. T. Englund, A novel pathway for glycan assembly: biosynthesis of the glycosyl-phosphatidylinositol anchor of the trypanosome variant surface glycoprotein. *Cell* **56**, 793-800 (1989).
3. M. A. J. Ferguson, G. W. Hart, T. Kinoshita, "Glycosylphosphatidylinositol Anchors" in Essentials of Glycobiology, A. Varki *et al.*, Eds. (Cold Spring Harbor Laboratory Press Copyright 2015-2017 by The Consortium of Glycobiology Editors, La Jolla, California. All rights reserved., Cold Spring Harbor (NY), 2015), 10.1101/glycobiology.3e.012, pp. 137-150.
4. M. Muniz, H. Riezman, Trafficking of glycosylphosphatidylinositol anchored proteins from the endoplasmic reticulum to the cell surface. *J Lipid Res* **57**, 352-360 (2016).
5. D. Hamburger, M. Egerton, H. Riezman, Yeast Gaa1p is required for attachment of a completed GPI anchor onto proteins. *J. Cell Biol.* **129**, 629-639 (1995).
6. M. Benghezal, A. Benachour, S. Rusconi, M. Aebi, A. Conzelmann, Yeast Gpi8p is essential for GPI anchor attachment onto proteins. *EMBO J.* **15**, 6575-6583 (1996).
7. T. Kinoshita, Biosynthesis and biology of mammalian GPI-anchored proteins. *Open Biol* **10**, 190290 (2020).
8. C. UniProt, UniProt: a hub for protein information. *Nucleic Acids Res* **43**, D204-212 (2015).
9. I. Kuki, Yukitoshi Takahashi, Shin Okazaki, Hisashi Kawawaki, Eiji Ehara, Norimitsu Inoue, Taroh Kinoshita and Yoshiko Murakami Case report on vitamin B6 responsive epilepsy due to inherited GPI deficiency. *Neurology* **81**, 1467-1469. (2013).
10. A. M. Almeida *et al.*, Hypomorphic promoter mutation in PIGM causes inherited glycosylphosphatidylinositol deficiency. *Nat Med* **12**, 846-851 (2006).
11. P. M. Krawitz *et al.*, Identity-by-descent filtering of exome sequence data identifies PIGV mutations in hyperphosphatasia mental retardation syndrome. *Nat Genet* **42**, 827-829 (2010).
12. G. Maydan *et al.*, Multiple congenital anomalies-hypotonia-seizures syndrome is caused by a mutation in PIGN. *J Med Genet* **48**, 383-389 (2011).
13. B. G. Ng *et al.*, Mutations in the glycosylphosphatidylinositol gene PIGL cause CHIME syndrome. *Am J Hum Genet* **90**, 685-688 (2012).
14. P. M. Krawitz *et al.*, Mutations in PIGO, a member of the GPI-anchor-synthesis pathway, cause hyperphosphatasia with mental retardation. *Am J Hum Genet* **91**, 146-151 (2012).
15. J. J. Johnston *et al.*, The phenotype of a germline mutation in PIGA: the gene somatically mutated in paroxysmal nocturnal hemoglobinuria. *Am J Hum Genet* **90**, 295-300 (2012).
16. M. Kvarnung *et al.*, A novel intellectual disability syndrome caused by GPI anchor deficiency due to homozygous mutations in PIGT. *J Med Genet* **50**, :521-528. (2013).
17. T. Chiyonobu, N. Inoue, M. Morimoto, T. Kinoshita, Y. Murakami, Glycosylphosphatidylinositol (GPI) anchor deficiency caused by mutations in PIGW is associated with West syndrome and

hyperphosphatasia with mental retardation syndrome. *J Med Genet* **51**, 203-207 (2014).

18. H. C. Martin *et al.*, Clinical whole-genome sequencing in severe early-onset epilepsy reveals new genes and improves molecular diagnosis. *Hum Mol Genet* **23**, 3200-3211 (2014).
19. B. Ilkovski *et al.*, Mutations in PIGY: expanding the phenotype of inherited glycosylphosphatidylinositol deficiencies. *Hum Mol Genet* 10.1093/hmg/ddv331 (2015).
20. P. Makrythanasis *et al.*, Pathogenic Variants in PIGG Cause Intellectual Disability with Seizures and Hypotonia. *Am J Hum Genet* **98**, 615-626 (2016).
21. S. Edvardson *et al.*, Mutations in the phosphatidylinositol glycan C (PIGC) gene are associated with epilepsy and intellectual disability. *J Med Genet* **54**, 196-201 (2017).
22. D. L. Johnstone *et al.*, Compound heterozygous mutations in the gene PIGP are associated with early infantile epileptic encephalopathy. *Hum Mol Genet* **26**, 1706-1715 (2017).
23. T. T. M. Nguyen *et al.*, Mutations in GPAA1, Encoding a GPI Transamidase Complex Protein, Cause Developmental Delay, Epilepsy, Cerebellar Atrophy, and Osteopenia. *Am J Hum Genet* **101**, 856-865 (2017).
24. T. T. M. Nguyen *et al.*, Mutations in PIGS, Encoding a GPI Transamidase, Cause a Neurological Syndrome Ranging from Fetal Akinesia to Epileptic Encephalopathy. *Am J Hum Genet* **103**, 602-611 (2018).
25. A. T. Pagnamenta *et al.*, A homozygous variant disrupting the PIGH start-codon is associated with developmental delay, epilepsy, and microcephaly. *Hum Mutat* **39**, 822-826 (2018).
26. A. Knaus *et al.*, Mutations in PIGU Impair the Function of the GPI Transamidase Complex, Causing Severe Intellectual Disability, Epilepsy, and Brain Anomalies. *Am J Hum Genet* **105**, 395-402 (2019).
27. Y. Murakami *et al.*, Mutations in PIGB Cause an Inherited GPI Biosynthesis Defect with an Axonal Neuropathy and Metabolic Abnormality in Severe Cases. *Am J Hum Genet* **105**, 384-394 (2019).
28. T. T. M. Nguyen *et al.*, Bi-allelic Variants in the GPI Transamidase Subunit PIGK Cause a Neurodevelopmental Syndrome with Hypotonia, Cerebellar Atrophy, and Epilepsy. *Am J Hum Genet* **106**, 484-495 (2020).
29. P. M. Krawitz *et al.*, PGAP2 Mutations, Affecting the GPI-Anchor-Synthesis Pathway, Cause Hyperphosphatasia with Mental Retardation Syndrome. *Am J Hum Genet* **92**, 584-589 (2013).
30. Y. Murakami *et al.*, Null mutation in PGAP1 impairing GPI-anchor maturation in patients with intellectual disability and encephalopathy. *Plos Genetics* **10**, e1004320 (2014).
31. M. Y. Howard MF, Pagnamenta AT, Haas CD, Fischer B, Hecht J, Keays DA, Knight SJL, Kölsch U, Krüger U, Leiz S, Maeda Y, Mitchell D, Mundlos S, Philipps JA, Robinson PN, Kini U, Taylor JC, Horn D, Kinoshita, Krawitz PM, Mutations in PGAP3 impair GPI-anchor maturation and lead to intellectual disability with hyperphosphatasia and additional phenotypic features. *Am J Hum Genet* **94**, 278-287 (2014).
32. M. Nozaki *et al.*, Developmental abnormalities of glycosylphosphatidylinositol-anchor-deficient embryos revealed by Cre/loxP system. *Lab. Invest.* **79**, 293-299 (1999).
33. Y. Hong *et al.*, Requirement of PIG-F and PIG-O for transferring phosphoethanolamine to the

third mannose in glycosylphosphatidylinositol. *J. Biol. Chem.* **275**, 20911-20919 (2000).

34. M. Takahashi *et al.*, PIG-B, a membrane protein of the endoplasmic reticulum with a large lumenal domain, is involved in transferring the third mannose of the GPI anchor. *EMBO J.* **15**, 4254-4261 (1996).
35. N. Shishioh *et al.*, GPI7 is the second partner of PIG-F and involved in modification of glycosylphosphatidylinositol. *J Biol Chem* **280**, 9728-9734 (2005).
36. M. Fujita *et al.*, GPI glycan remodeling by PGAP5 regulates transport of GPI-anchored proteins from the ER to the Golgi. *Cell* **139**, 352-365 (2009).
37. J. J. Zhao *et al.*, Reduced cell surface levels of GPI-linked markers in a new case with PIGG loss of function. *Hum Mutat* **38**, 1394-1401 (2017).
38. R. Oriol, I. Martinez-Duncker, I. Chantret, R. Mollicone, P. Codogno, Common origin and evolution of glycosyltransferases using Dol-P-monosaccharides as donor substrate. *Mol. Biol. Evol.* **19**, 1451-1463 (2002).
39. B. W. Taron, P. A. Colussi, J. M. Grimme, P. Orlean, C. H. Taron, Human Smp3p adds a fourth mannose to yeast and human glycosylphosphatidylinositol precursors in vivo. *J. Biol. Chem.* **279**, 36083-36092 (2004).
40. T. Kitamura, N. Sato, K. Arai, A. Miyajima, Expression cloning of the human IL-3 receptor cDNA reveals a shared beta subunit for the human IL-3 and GM-CSF receptors. *Cell* **66**, 1165-1174 (1991).
41. T. Hirata *et al.*, Identification of a Golgi GPI-N-acetylgalactosamine transferase with tandem transmembrane regions in the catalytic domain. *Nat Commun* **9**, 405 (2018).
42. Y. Wang *et al.*, Cross-talks of glycosylphosphatidylinositol biosynthesis with glycosphingolipid biosynthesis and ER-associated degradation. *Nat Commun* **11**, 860 (2020).
43. B. C. Searle, Scaffold: a bioinformatic tool for validating MS/MS-based proteomic studies. *Proteomics* **10**, 1265-1269 (2010).
44. M. A. Ferguson, S. W. Homans, R. A. Dwek, T. W. Rademacher, Glycosyl-phosphatidylinositol moiety that anchors Trypanosoma brucei variant surface glycoprotein to the membrane. *Science* **239**, 753-759 (1988).
45. S. Moody-Haupt, J. H. Patterson, D. Mirelman, M. J. McConville, The major surface antigens of Entamoeba histolytica trophozoites are GPI-anchored proteophosphoglycans. *J Mol Biol* **297**, 409-420 (2000).
46. G. Heimer *et al.*, Netrin-G2 dysfunction causes a Rett-like phenotype with areflexia. *Hum Mutat* **41**, 476-486 (2020).
47. C. M. Dias *et al.*, Homozygous Missense Variants in NTNG2, Encoding a Presynaptic Netrin-G2 Adhesion Protein, Lead to a Distinct Neurodevelopmental Disorder. *Am J Hum Genet* **105**, 1048-1056 (2019).
48. M. Minor, K. P. Alcedo, R. A. Battaglia, N. T. Snider, Cell type- and tissue-specific functions of ecto-5'-nucleotidase (CD73). *Am J Physiol Cell Physiol* **317**, C1079-C1092 (2019).
49. J. Yu *et al.*, The affected gene underlying the class K glycosylphosphatidylinositol (GPI) surface protein defect codes for the GPI transamidase. *Proc. Natl. Acad. Sci. USA* **94**, 12580-12585 (1997).

50. B. Eisenhaber, S. Eisenhaber, T. Y. Kwang, G. Gruber, F. Eisenhaber, Transamidase subunit GAA1/GPAA1 is a M28 family metallo-peptide-synthetase that catalyzes the peptide bond formation between the substrate protein's omega-site and the GPI lipid anchor's phosphoethanolamine. *Cell Cycle* **13**, 1912-1917 (2014).
51. K. Ohishi, N. Inoue, T. Kinoshita, PIG-S and PIG-T, essential for GPI anchor attachment to proteins, form a complex with GAA1 and GPI8. *EMBO J.* **20**, 4088-4098. (2001).
52. Y. Hong *et al.*, Human PIG-U and yeast Cdc91p are the fifth subunit of GPI transamidase that attaches GPI-anchors to proteins. *Mol Biol Cell* **14**, 1780-1789 (2003).
53. M. Fujita, T. Yoko-o, M. Okamoto, Y. Jigami, GPI7 involved in glycosylphosphatidylinositol biosynthesis is essential for yeast cell separation. *J Biol Chem* **279**, 51869-51879 (2004).
54. S. Tanaka, Y. Maeda, Y. Tashima, T. Kinoshita, Inositol deacylation of glycosylphosphatidylinositol-anchored proteins is mediated by mammalian PGAP1 and yeast Bst1p. *J. Biol. Chem.* **279**, 14256-14263 (2004).
55. W. L. Roberts, J. J. Myher, A. Kuksis, M. G. Low, T. L. Rosenberry, Lipid analysis of the glycoinositol phospholipid membrane anchor of human erythrocyte acetylcholinesterase. Palmitoylation of inositol results in resistance to phosphatidylinositol-specific phospholipase C. *J Biol Chem* **263**, 18766-18775 (1988).
56. Y. S. Liu *et al.*, N-Glycan-dependent protein folding and endoplasmic reticulum retention regulate GPI-anchor processing. *J Cell Biol* **217**, 585-599 (2018).
57. L. Cong *et al.*, Multiplex genome engineering using CRISPR/Cas systems. *Science* **339**, 819-823 (2013).
58. F. Meier *et al.*, Online Parallel Accumulation-Serial Fragmentation (PASEF) with a Novel Trapped Ion Mobility Mass Spectrometer. *Mol Cell Proteomics* **17**, 2534-2545 (2018).
59. F. Meier *et al.*, Parallel Accumulation-Serial Fragmentation (PASEF): Multiplying Sequencing Speed and Sensitivity by Synchronized Scans in a Trapped Ion Mobility Device. *J Proteome Res* **14**, 5378-5387 (2015).
60. G. H. Lee *et al.*, PGAP6, a GPI-specific phospholipase A2, has narrow substrate specificity against GPI-anchored proteins. *J Biol Chem* **295**, 14501-14509 (2020).
61. J. A. Vizcaíno *et al.*, 2016 update of the PRIDE database and its related tools. *Nucleic Acids Res* **44**, D447-456 (2016).

Figure legends

Figure 1. Complete silencing of residual expression of CD59 and DAF GPI-APs in *PIGO*-KO HEK293 cells by knocking out *PIGG* (*PIGO*-*PIGG*-DKO).

A. Regular levels of CD59 and DAF in *PIGG*-KO cells as determined by FACS analysis. B. *PIGO*-KO cells expressing low levels of CD59 and DAF, and restored by transfection of *PIGO* cDNA. C. Complete removal of residual expression of CD59 and DAF in *PIGO*-KO cells by further knockout of *PIGG* (*PIGO*-*PIGG*-DKO). D. Resistance of CD59 and DAF expressed in *PIGO*-KO cells to PI-PLC treatment. Isotype control, isotypic cells stained with non-matching antibody, as negative control.

Figure 2. Complete silencing of residual expression of synthesized in *PIGB*-KO HEK293 cells by knocking out *PIGG* (*PIGB*-*PIGG*-DKO).

A. *PIGB*-KO cells expressing low levels of CD59 and DAF, and restored by transfection of *PIGB* cDNA. B. Further knockout of *PIGZ* showing no decrease CD59 and DAF expression in *PIGB*-KO (*PIGB*-*PIGZ*-DKO) cells. C. Complete removal of residual expression of CD59 and DAF in *PIGB*-KO cells by further knockout of *PIGG* (*PIGB*-*PIGG*-DKO). D. Sensitivity of CD59 and partial sensitivity of DAF expressed in *PIGB*-KO cells, to PI-PLC treatment.

Figure 3. Mass spectrometric analysis of trypsin fragments of CD59 expressed in wild

type HEK293 cells.

A. Schematic MS/MS profile showing the CD59 C-terminal eleven amino acids linked to the typical GPI glycan, EthN-P-Man-Man- (EthN-P-)(HexNAc-)Man-GlcN-Ino-P. B. The MS/MS profile of a major precursor ion of *m/z* 1367.97^{2+} corresponding to the glycan shown in A.

Figure 4. Mass spectrometric analysis of trypsin fragments of CD59 expressed in *PIGB*-KO HEK293 cells.

A, Schematic MS/MS profile showing the CD59 C-terminal eleven amino acids linked to a GPI glycan with only two mannoses. B. MS/MS analysis of fragment ions *m/z* 689^{+} corresponding to -P-Man-(EthN-P-)Man-GlcN and *m/z* 1948^{+} corresponding to (11 amino acids)-EthN-P-Man-(EthN-P-)Man indicating CD59 C-terminus attachment to EthN-P linked to the second mannose.

Figure 5. Protein attachment to EthN-P linked to the second mannose found in a small fraction of CD59 in wild type HEK293 cells.

A. Schematic MS/MS profile of CD59 C-terminal eleven amino acids linked to the second mannose of a GPI glycan. B. C. MS/MS analysis of fragment ions of *m/z* 689^{+} and 1948^{+} (diagnostic for protein attachment to EthN-P on the second mannose), found in approximately 10% of precursor ions of *m/z* 1367.47^{2+} (11 amino acids plus GPI

consisting of three mannoses, two EthN-P, GlcN, HexNAc, inositol and phosphate), indicating protein attachment to EthN-P on the second mannose.

Figure 6. Flowchart of method for purification and fragmentation of GPI-APs for MS analysis.

Cells are lysed at 4°C in Triton X114, followed by low speed centrifugation and warming up of supernatant to 37 °C for phase separation. The detergent phase is collected and cold buffer (10 mM Tris-HCl, pH 7.4, 150 mM NaCl, 5 mM EDTA, proteinase inhibitor) added to dilute the TritonX-114, followed by PI-PLC treatment at 4°C for 90 minutes, and a second phase separation. PI-PLC-sensitive GPI-APs fragments stay solubilized in the aqueous phase, while PI-PLC-resistant GPI-APs stay into the detergent phase. GPI-APs fragments are concentrated by acetone precipitation and centrifugation, and subjected to MS analysis.

Figure 7. Expression levels of various GPI-APs in *PIGG*-KO cells compared to levels in the wild type HEK293 cells, determined by FACS analysis.

A. Expression levels of various GPI-APs in different clones of *PIGG*-KO HEK293 cells. Levels of NT5E in *PIGG*-KO clones #4, #10, #17, #19 and wild type cells are 575, 910, 696, 530 and 1548 while those of EphrinA5 in clones #4, #17, #19 and wild type cells are 1431, 2080, 1868 and 3336, respectively. B. Expression levels of GPI-APs in *PIGG*-

KO clone #19 cells stably transfected with *PIGG* cDNA compared to levels in empty vector transfected cells. Fluorescent intensities of NT5E in *PIGG* cDNA and in vector transfected cells were 1332 and 886, respectively.

Figure 8. PIGG dependent expression of GPI-APs (FACS analysis).

A. Expression levels of different GPI-APs in *PIGG*-KO HEK293 cells transiently co-transfected with *PIGG* cDNA or empty vector. Vertical bars represent% of levels of GPI-APs expression in *PIGG* cDNA rescued *PIGG*-KO cells relative to those in non-rescued *PIGG*-KO cells. B. FACS analysis of HA tagged *NTNG2* and FLAG tagged *CD55* co-transfected with *PIGG* cDNA or empty vector to *PIGG*-KO cells. Levels of NTNG2 in *PIGG*-KO cells and in *PIGG* rescued cells are 639 and 3426, while those of DAF in *PIGG*-KO cells and in *PIGG* rescued cells are 562 and 599, respectively.

Figure 9. Functional activity assay of R669C mutant *PIGG* cDNA on CD59 and DAF GPI-APs expression in *PIGO/PIGG*-DKO cells (FACS analysis).

PIGO/PIGG-DKO HEK293 cells transfected with wild type or R669C mutant *PIGG* cDNA with GST tagged C-terminal. The R669C-*PIGG* cDNA - partially restore the expression of CD59 while very little of DAF (blue line) as compared the restoration level promoted by the unmutated *PIGG* cDNA (red line).

Figure 1

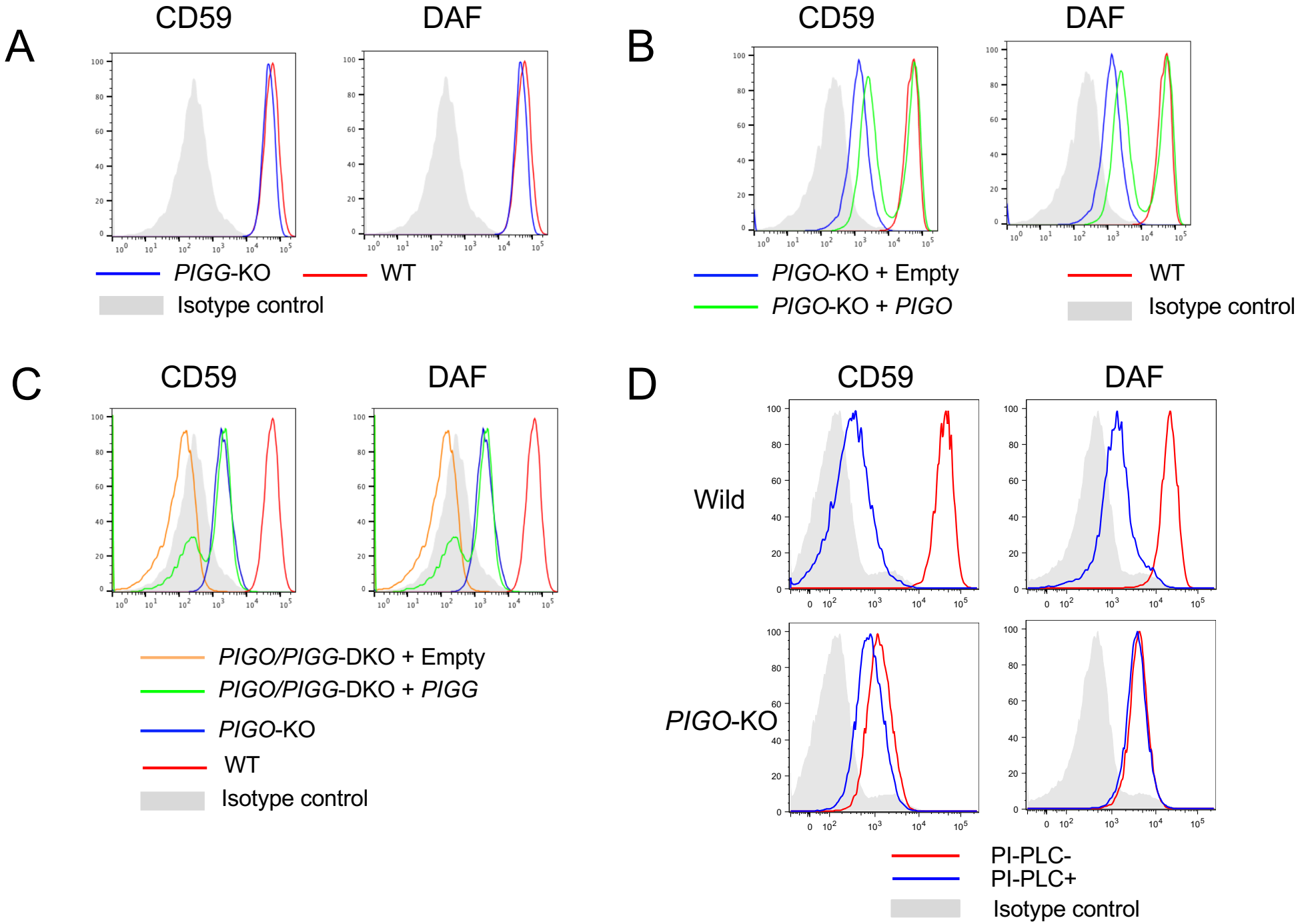
A
CD59
DAF
PIGG-KO
WT
Isotype control
B
CD59
DAF
PIGO-KO + Empty
PIGO-KO + PIGO
WT
Isotype control
C
CD59
DAF
PIGO/PIGG-DKO + Empty
PIGO/PIGG-DKO + PIGG
PIGO-KO
WT
Isotype control
D
CD59
DAF
Wild
PIGO-KO
PI-PLC-
PI-PLC+
Isotype control

Figure 2

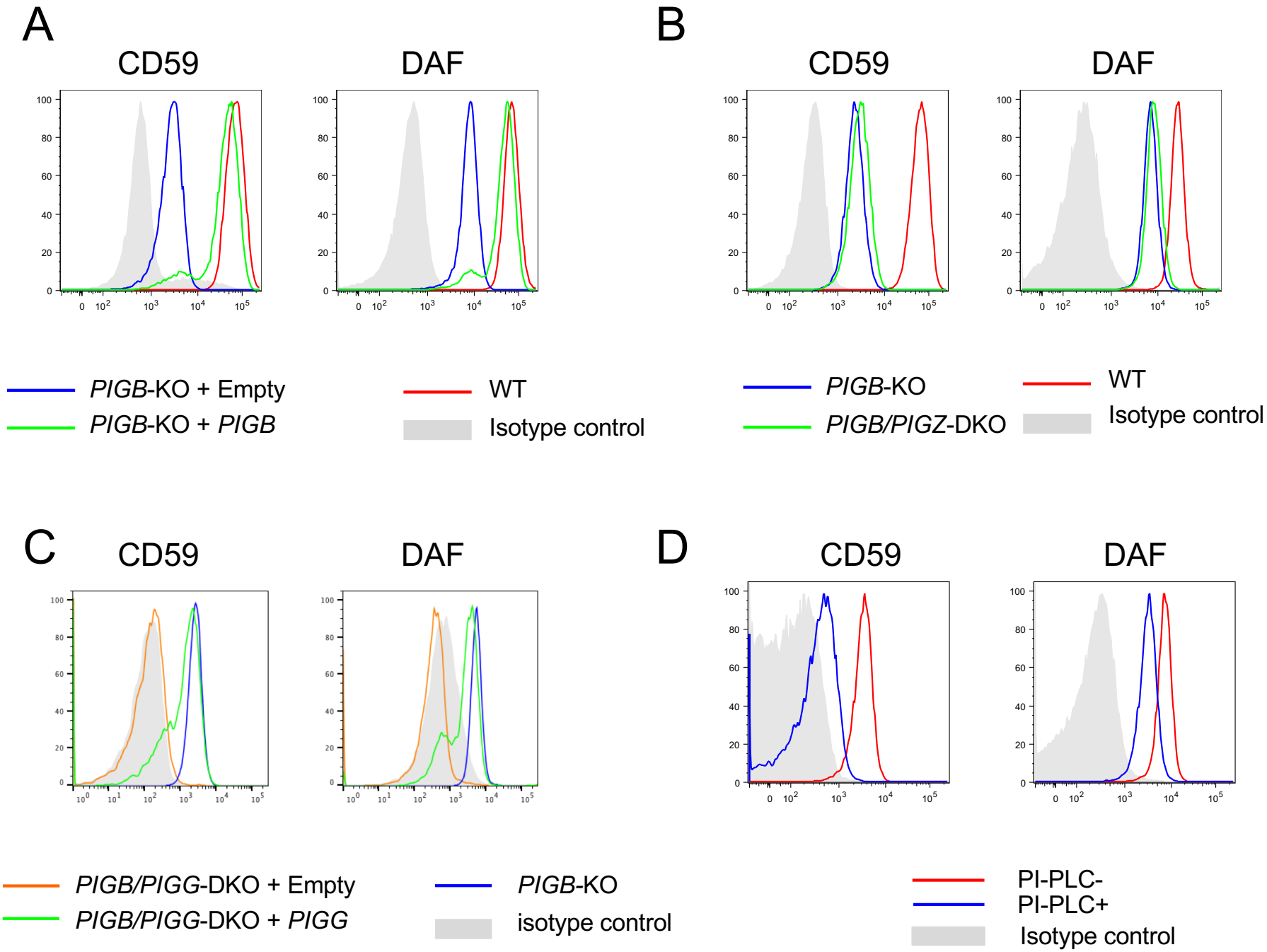
A
CD59
DAF
B
CD59
DAF
C
CD59
DAF
D
CD59
DAF
PIGB-KO + Empty
PIGB-KO + *PIGB*
WT
Isotype control
PIGB-KO
PIGB/PIGZ-DKO
WT
Isotype control
PIGB/PIGG-DKO + Empty
PIGB/PIGG-DKO + *PIGG*
PIGB-KO
isotype control
PI-PLC-
PI-PLC+
Isotype control

Figure 3

A

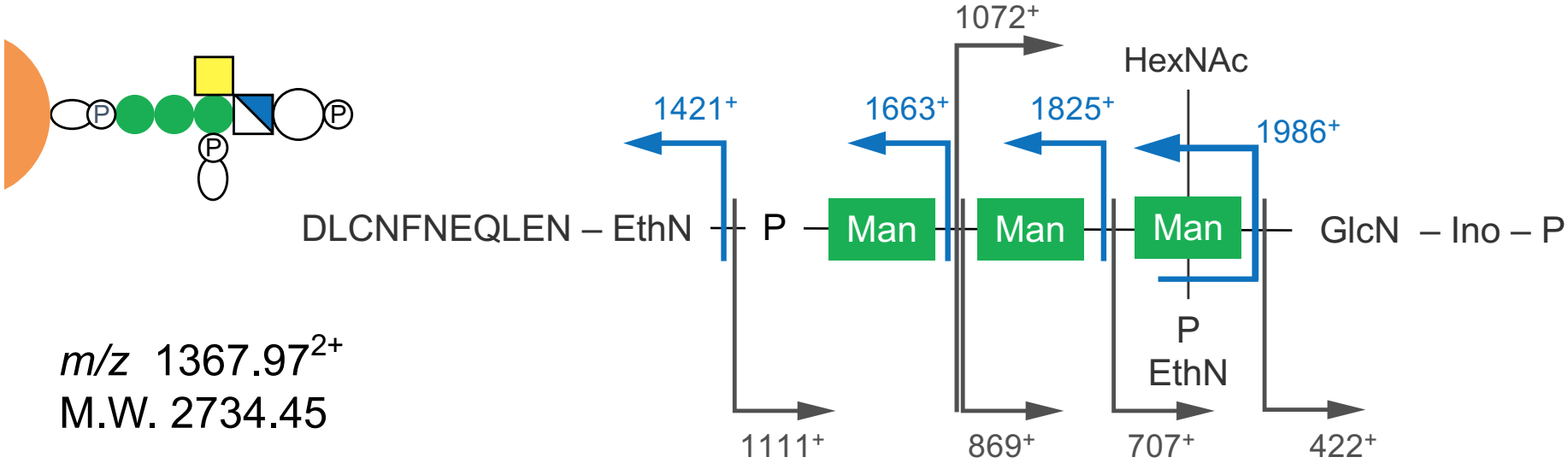
P
P
P
1072+
HexNAc
1421+
1663+
1825+
1986+
DLCNFNEQLEN – EthN
P
Man
Man
Man
GlcN – Ino – P
P
EthN
m/z 1367.97 2+
M.W. 2734.45
1111+
869+
707+
422+

B

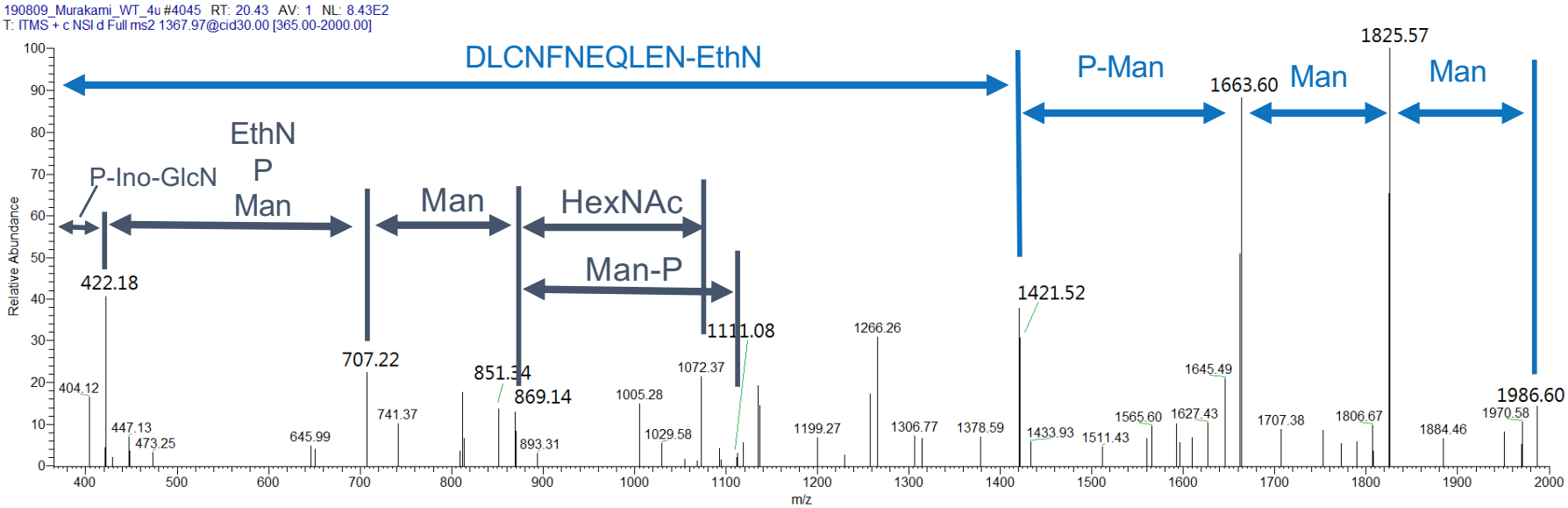
190809_Murakami_WT_4u #4045 RT: 20.43 AV: 1 NL: 8.43E2
T: ITMS + c NSI d Full ms2 1367.97@cid30.00 [365.00-2000.00]
DLCNFNEQLEN-EthN
P-Man
Man
Man
EthN
P
Man
P-Ino-GlcN
Man
HexNAc
Man-P
Relative Abundance
m/z
422.18
707.22
851.34
869.14
1111.08
1072.37
1005.28
1029.58
1266.26
1421.52
1663.60
1825.57
1986.60
404.12
447.13
473.25
645.99
741.37
893.31
1199.27
1306.77
1378.59
1433.93
1511.43
1565.60
1627.43
1645.49
1707.38
1806.67
1884.46
1970.58

Figure 4

A

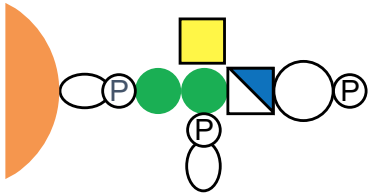

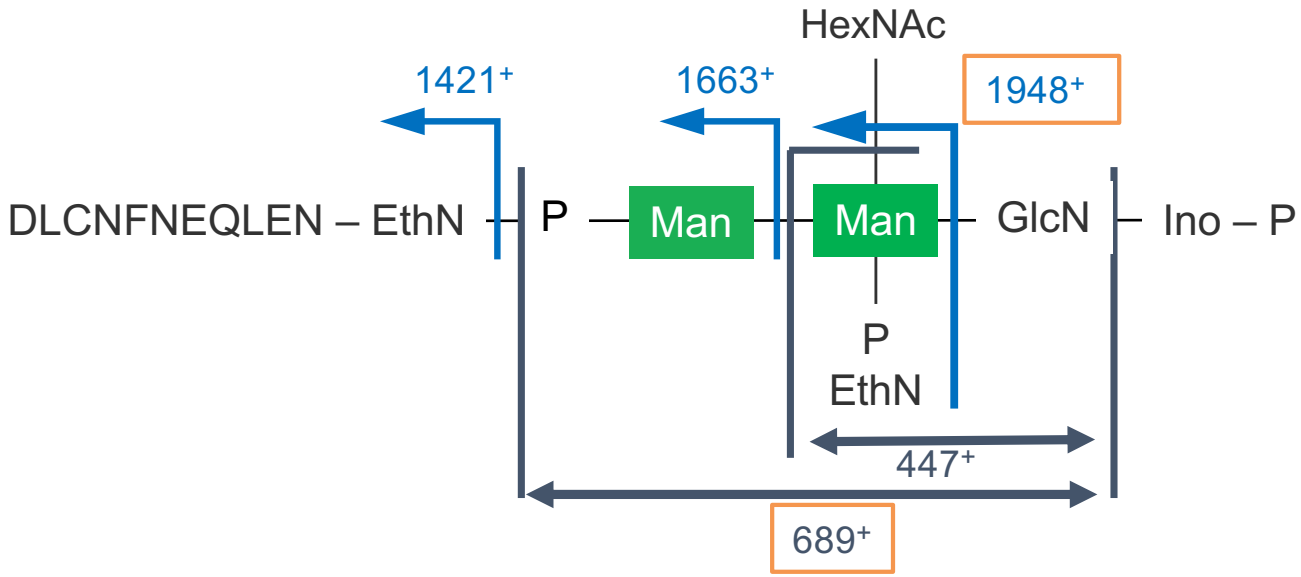

m/z 1286.44^{2+}
M.W. 2572.31

B

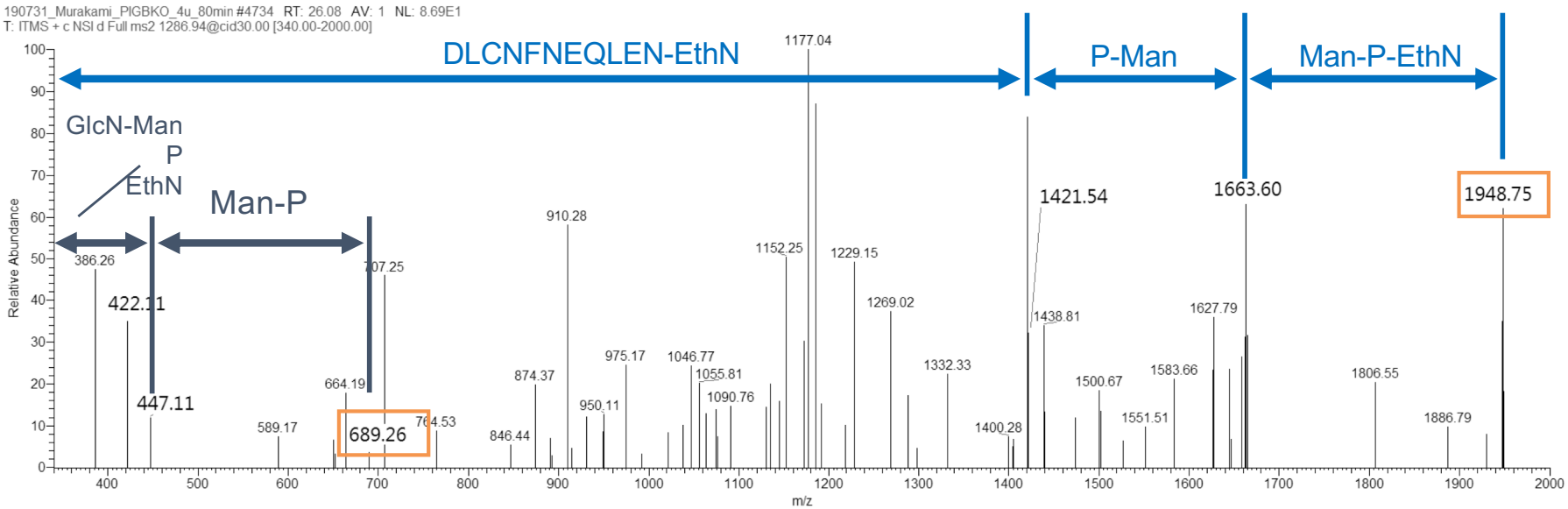

Figure 5

A

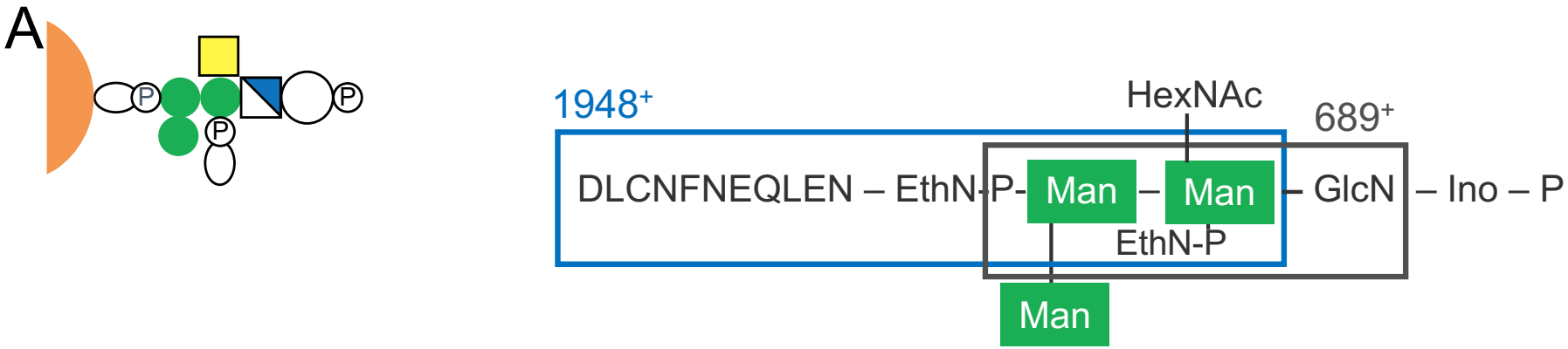
P
P
P
1948+
HexNAc
689+
DLCNFNEQLEN – EthN-P- Man – Man – GlcN – Ino – P
EthN-P
Man

B

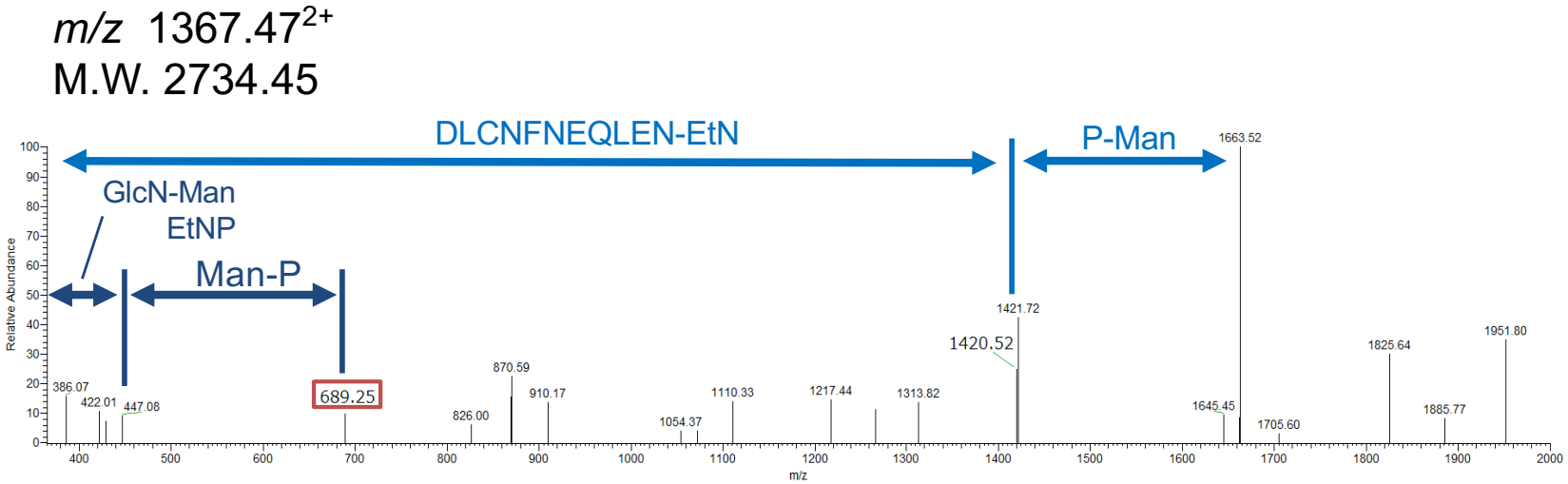
m/z 1367.47 2+
M.W. 2734.45
DLCNFNEQLEN-EtN
P-Man
GlcN-Man
EtNP
Man-P
Relative Abundance
m/z
689.25
1421.72
1420.52
1663.52
1825.64
1951.80
1885.77
1705.60
1645.45
1313.82
1217.44
1110.33
1054.37
910.17
870.59
826.00
386.07
422.01
447.08

C

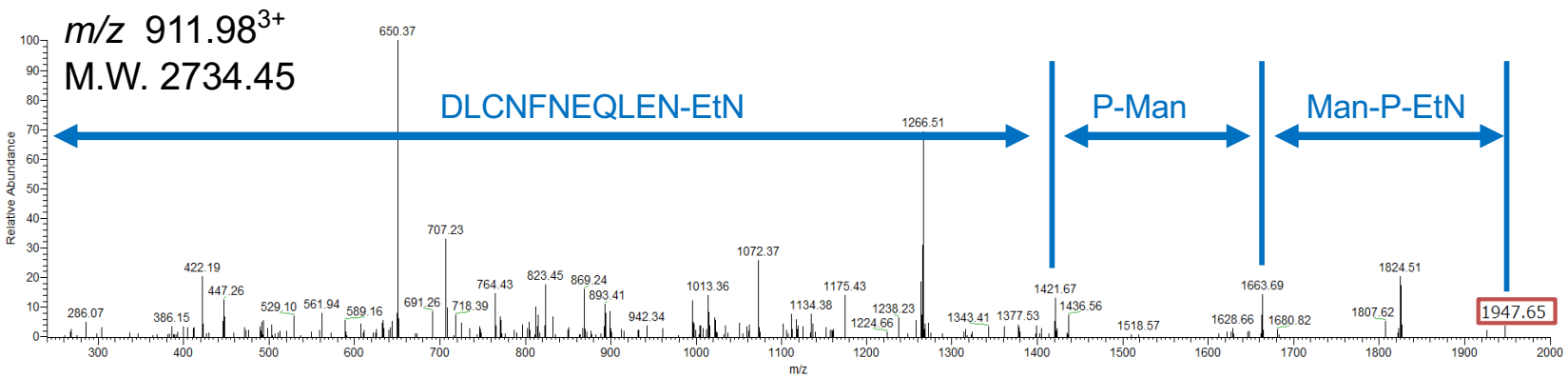
m/z 911.98 3+
M.W. 2734.45
DLCNFNEQLEN-EtN
P-Man
Man-P-EtN
Relative Abundance
m/z
650.37
1266.51
707.23
1072.37
1421.67
1663.69
1824.51
1947.65
1436.56
1807.62
1680.82
1628.66
1518.57
1377.53
1343.41
1224.66
1238.23
1175.43
1134.38
1013.36
942.34
893.41
869.24
823.45
764.43
718.39
691.26
589.16
561.94
529.10
447.26
422.19
386.15
286.07

Figure 6

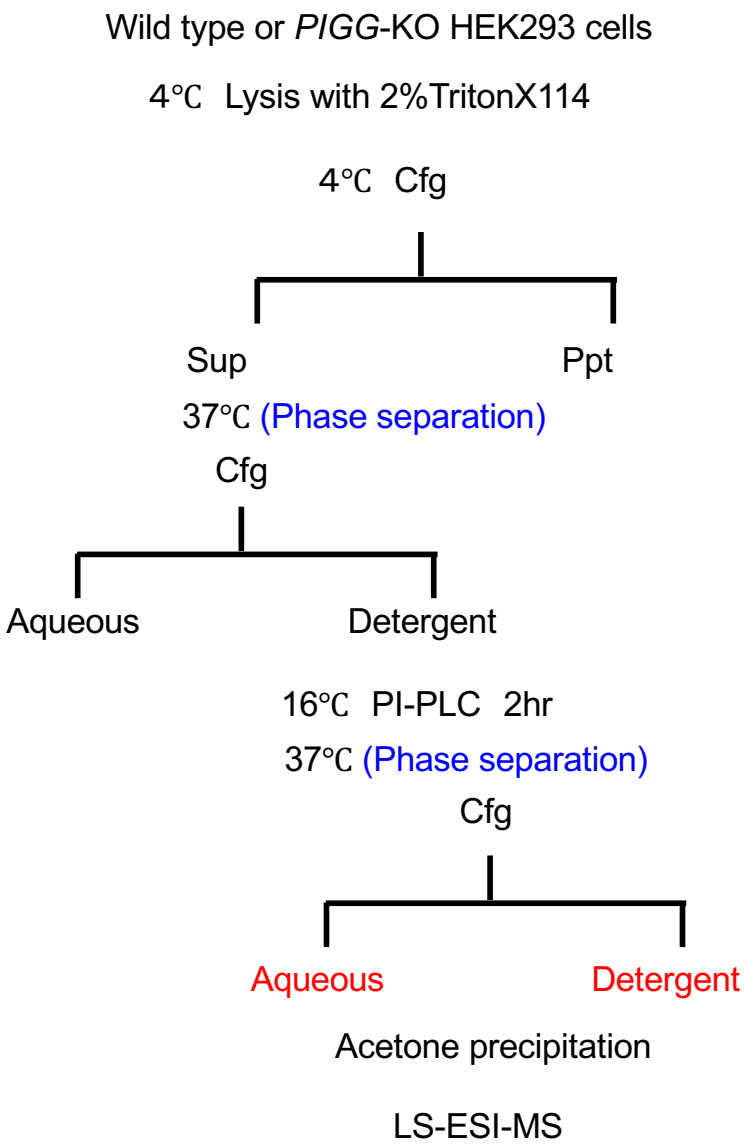
Wild type or *PIGG*-KO HEK293 cells
4℃ Lysis with 2%TritonX114
4℃ Cfg
Sup
Ppt
37℃ (Phase separation)
Cfg
Aqueous
Detergent
16℃ PI-PLC 2hr
37℃ (Phase separation)
Cfg
Aqueous
Detergent
Acetone precipitation
LS-ESI-MS

Figure 7

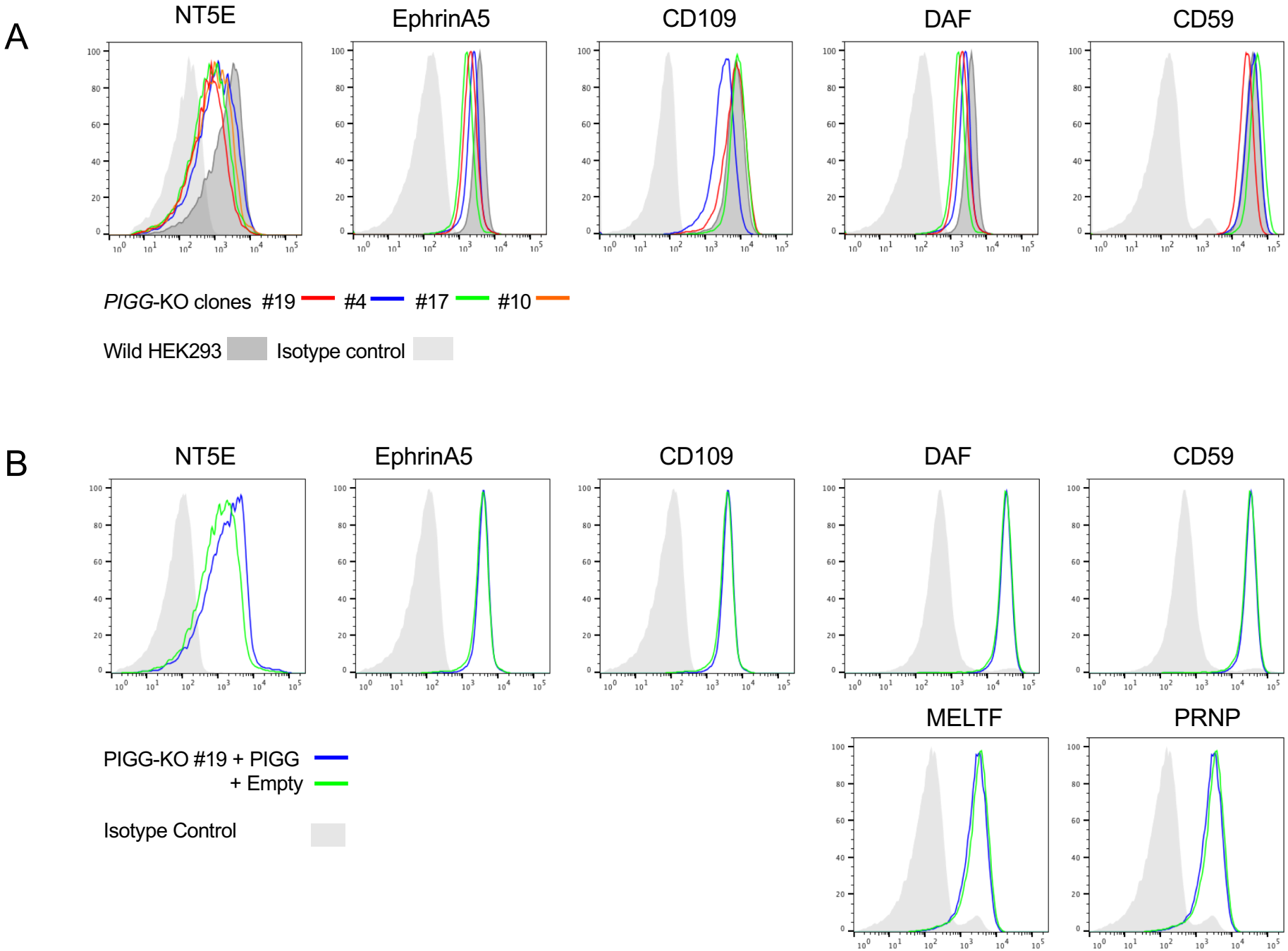
A
NT5E
EphrinA5
CD109
DAF
CD59
PIGG-KO clones #19 #4 #17 #10
Wild HEK293
Isotype control
B
NT5E
EphrinA5
CD109
DAF
CD59
MELTF
PRNP
PIGG-KO #19 + PIGG
+ Empty
Isotype Control

Figure 8

A.

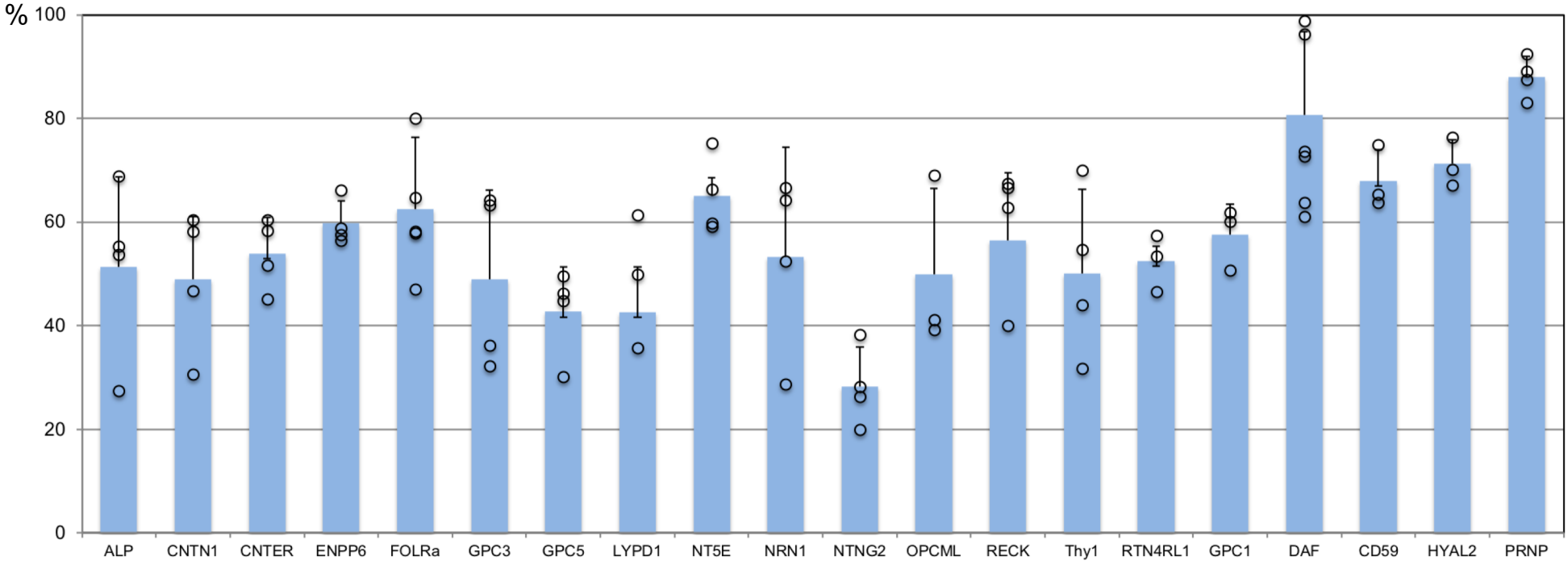
%
100
80
60
40
20
0
ALP
CNTN1
CNTER
ENPP6
FOLRa
GPC3
GPC5
LYPD1
NT5E
NRN1
NTNG2
OPCML
RECK
Thy1
RTN4RL1
GPC1
DAF
CD59
HYAL2
PRNP

B.

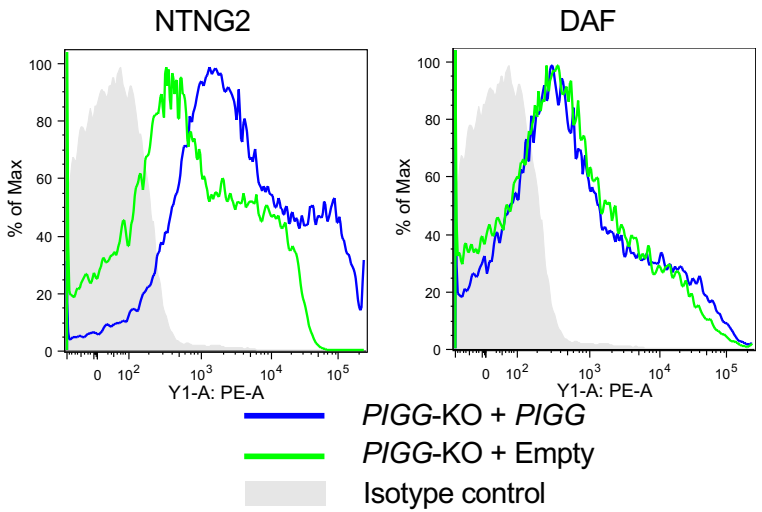
NTNG2
DAF
% of Max
Y1-A: PE-A
PIGG-KO + PIGG
PIGG-KO + Empty
Isotype control

Figure 9

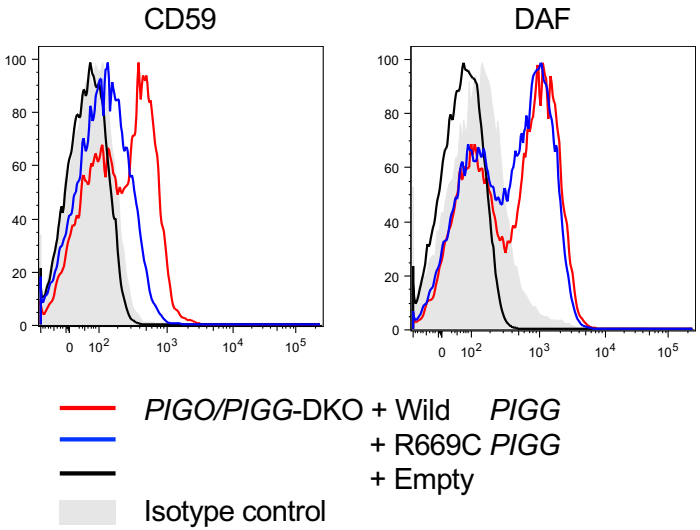
CD59
DAF
100
80
60
40
20
0
0
10^2
10^3
10^4
10^5
PIGO/PIGG-DKO + Wild *PIGG*
+ R669C *PIGG*
+ Empty
Isotype control